

<https://doi.org/10.1038/s41534-025-01028-7>

Discovery of entanglement generation by elastic collision to realise the original Einstein-Podolsky-Rosen thought experiment



Roman Schnabel ✉

The amazing quantum effect of ‘entanglement’ was discovered in the 1935 thought experiment by Albert Einstein, Boris Podolsky and Nathan Rosen (‘EPR’)¹. The ensuing research opened up fundamental questions and led to experiments that proved that quantum theory cannot be completed by local hidden variables^{2–4}. Remarkably, EPR did not discuss how to create the entanglement in their thought experiment. Here I add this part. What is required in the original EPR thought experiment is a simple elastic particle collision, an unbalanced mass ratio of e.g. 1:3 and initial states that are position and momentum squeezed, respectively. In the limiting case of infinite squeeze factors, the measurement of the position or momentum of one particle allows an absolutely precise conclusion to be drawn about the value of the same quantity of the other particle. The EPR idea has never been tested in this way. I outline a way to do this.

In their seminal 1935 paper¹, Einstein, Podolsky and Rosen presented a thought experiment with two systems that had interacted with each other in the past but no longer do. The past interaction had ‘entangled’ the systems, a term introduced by Erwin Schrödinger in his response⁵. EPR were finally specific in the presentation of their thought experiment. They considered the entanglement of the momenta and positions (coordinates) of two particles, which I will refer to here as ‘A’ and ‘B’. For a statistical analysis, the entanglement was prepared many times in exactly the same way. The successive measurements on particle A (its location $\hat{x}_{A,i}$ or its momentum $\hat{p}_{A,j}$) as well as those on particle B ($\hat{x}_{B,i}$ or $\hat{p}_{B,j}$) nevertheless resulted in different values due to quantum uncertainty.

The core of the EPR thought experiment was the discovery of correlations *within* the spread of the uncertainty distributions. Every two simultaneous position measurements ($x_{A,i}$ and $x_{B,i}$) did provide varying values but they were always mutually identical. Two simultaneous momentum measurements ($p_{A,j}$ and $p_{B,j}$) also provided varying values, but always had a sum of precisely zero. The fact that any quantum uncertainty disappears in the *relative* measurements on a pair has led EPR to question whether quantum theory is complete¹. Many other quantum physicists did not question this. Schrödinger saw nevertheless a paradox in the EPR thought experiment⁵.

EPR did not describe in their thought experiment how the position/momentum entanglement of two particles could be realised. Starting in the

1970s, there are now a large number of EPR experiments that realise the EPR paradox with different observables and different quantum systems. These include entangled systems of definite photon numbers^{2,4,6}, followed by conceptionally similar experiments with the occupation numbers of internal states of trapped ions⁷, of two atoms and a cavity mode⁸, of the stretch modes of two separated atomic mechanical oscillators⁹, of electron spin oscillators in defects of two separated crystals¹⁰, and of phonon number excitations of two artificially engineered mechanical oscillators¹¹.

A second kind of EPR experiments has used *indefinite* numbers of quanta and produced entanglement of the position-like and momentum-like observables, in particular the amplitude and phase quadratures amplitudes \hat{X} and \hat{Y} . Their continuous-variable probability density distributions of eigen values obey the Heisenberg uncertainty relation $\Delta^2 \hat{X} \cdot \Delta^2 \hat{Y} \geq 1/16$, where the Δ^2 denote variances. Also here, the first demonstrated systems were optical, namely laser beams having well-defined optical frequencies, polarisations, and transverse modes^{12,13}. Another example is EPR experiments with the transverse position and momentum of optical fields in the context of imaging^{14,15}. As an example of systems with mass, the position- and momentum-like projections of the collective spin of atomic clouds were entangled, e.g. clouds of about 10^{12} caesium atoms¹⁶ or about 10^4 rubidium atoms¹⁷.

Here I present the previously unknown interaction of how two free particles get entangled with respect to their real positions and momenta,

namely those of their centre of mass motion, to realise the source for the original EPR thought experiment. It is an elastic collision in one dimension, where the bodies must have unequal mass and are initially in position- and momentum-uncertainty-squeezed Gaussian states, respectively. I show that the entangling process is a natural consequence of the existence of quantum uncertainty and conservation of energy and momentum. I use a semi-classical approach that neglects the interference of the uncertainty ranges (during the collision). I consider this to be well-founded, as significant interference only occurs when very similar wave functions overlap. In the case considered here, neither the masses of the systems nor their quantum states are the same. The *measurement* of the positions and momenta only takes place when the wave functions are clearly separated again by the kinetics, so that my model is not subject to a semi-classical approximation during the measurement. Note that the (Bargmann) mass-superselection rule does not apply, because the masses of the particles are no dynamical variables¹⁸. I propose to put the EPR thought experiment into reality with precisely those systems and system observables originally discussed by EPR using an ensemble of a large number of identically prepared position/momentum entangled pairs of freely propagating atoms or ions.

Gaussian quantum uncertainties

The emergence of motional (position/momentum) EPR entanglement of two particles in Gaussian quantum states through an elastic collision is illustrated in Fig. 1. The equivalent *phase space* description is presented by the figure of the supplementary information.

States with Gaussian quantum uncertainties can minimize Heisenberg's uncertainty relation^{19–22}. The most prominent pair of non-commuting observables whose eigen value spectrums can show a Gaussian distribution are the position \hat{x} and the momentum \hat{p} , the two observables of motion. With $\Delta^2\hat{x}$ and $\Delta^2\hat{p}$ being the variances of their quantum uncertainties, Heisenberg's uncertainty relation reads

$$\Delta^2\hat{x} \cdot \Delta^2\hat{p} \geq \frac{\hbar^2}{4}, \quad (1)$$

where \hbar is the reduced Planck constant.

Two systems 'A' and 'B', both of which must generally obey inequality (1), are in a position/moment entangled state, if the measurement values on

the individual systems reveal correlations tighter than the minimum uncertainty product in inequality (1). A sufficient and necessary criterion for the most generic form of Gaussian entanglement, which is also called 'inseparability', is given in^{23,24}. If the measurement values from one system allow for the inference of the values of the same observable from the second system to better than the second system's minimum uncertainty product $\hbar^2/4$, then we speak about 'EPR entanglement'^{13,25–27}. EPR entangled systems are always also inseparable, while the converse of this statement does not apply^{13,26}. EPR entanglement corresponds to the correlations found in the original thought experiment of Einstein, Podolsky and Rosen¹.

Squeezed motional states of a particle

A particle in a harmonic potential being in its motional ground state has position and momentum expectation values of $\langle\hat{x}\rangle = \langle\hat{p}\rangle = 0$, defined with respect to the minimum of the trapping potential. Precise measurements performed on identical such particles, however, map out the respective quantum uncertainties around zero. They have a continuous Gaussian spectrum of 'eigen values'. The variances of the measured eigen values read

$$\Delta^2\hat{x} = \frac{\hbar}{2m\Omega}, \Delta^2\hat{p} = \frac{\hbar m\Omega}{2}, \quad (2)$$

where Ω is the trapping angular frequency. If the trapping frequency is quickly reduced, its state becomes position squeezed: The (old) position uncertainty is smaller than the ground state's position uncertainty in the new potential. Such a state is represented by a vertically aligned ellipse in the position/momentum phase space, see the left ellipse in the figure of the supplementary information. If the trapping frequency is quickly increased, the state becomes momentum squeezed, see the lower ellipse in the same figure. If the trapping potential turns to a flat potential, the particle gradually increases its squeezed position uncertainty towards infinity and reduces its anti-squeezed momentum uncertainty to zero. After an infinitely long time, the state of the particle reaches the new ground state with infinitely extended position uncertainty and precise momentum. This is the well-known 'free evolution of a Gaussian wave packet' that can be found in textbooks on quantum physics. Figure 1 and the figure of the supplementary information, however, show entanglement generation on a time scale that is much shorter

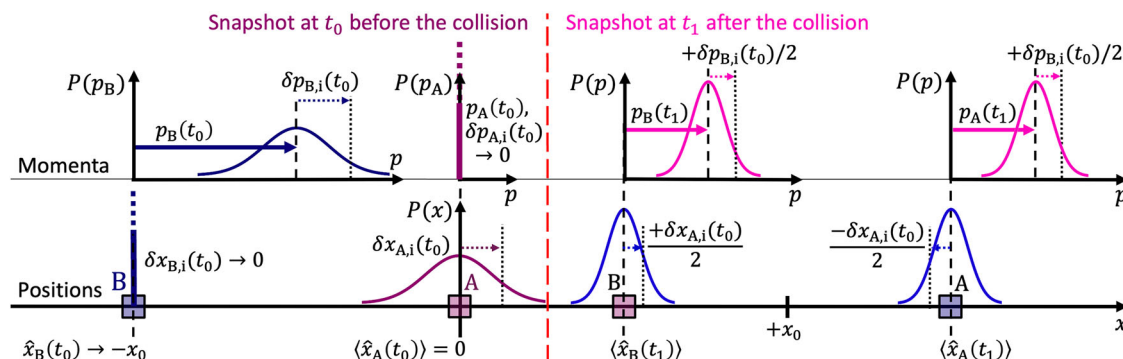


Fig. 1 | EPR entanglement from elastic collision. – Before the collision, at time t_0 (left half), particle A with mass m_A rests at $\langle x_A(t_0) \rangle = 0$ with a large Gaussian position uncertainty and negligible, strongly squeezed momentum uncertainty. The entanglement is produced by a single collision with particle B having the mass $m_B = 3m_A$, a high momentum $\langle \hat{p}_B(t_0) \rangle \gg \Delta \hat{p}_B(t_0) \gg 0$, and a position $\hat{x}_B(t_0) = -x_0$ with negligible, strongly squeezed position uncertainty. After the collision, at time t_1 (right half), measurements are performed. The two masses have the same momentum $\langle \hat{p}_B(t_1) \rangle = \langle \hat{p}_A(t_1) \rangle$ due to the mass ratio 1:3 and the conservations of momentum and energy. The momenta are even identical for any individual ensemble measurement 'i' since the momentum uncertainties (almost) exclusively originate from particle B. The measured values $\langle \hat{p}_{A,B}(t_1) \rangle + \delta p_{A,B,i}(t_1)$ (vertical dashed lines in the Gaussian distributions top right) are always identical, i.e. the differential values show no quantum uncertainty. The momentum uncertainties of the two particles are quantum

correlated. The initial position uncertainty $\Delta \hat{x}_A(t_0) \gg 0$ gets also distributed onto both particles. The right half of the Gaussian uncertainty corresponds to a statistically later collision, which results in a later establishment of new velocities. The collision halves the velocity of mass B, and mass A is accelerated to 3/2 of the initial velocity of B. The position uncertainty of A is therefore mirrored at its centre line and compressed by a factor of 1/2 due to A's uncertain initial position, see Eq. (11) while B takes over the other half of A's position uncertainty without a change of sign (see supplement). In conclusion, the position uncertainties of particles A and B after the collision are quantum anti-correlated. By measuring either A or B we are in a position to predict with certainty, and without in any way disturbing the second system either the value of the quantity $[x]$ or the value of the quantity $[p]$. My complemented version of the EPR thought experiment makes obvious that the description by the wave function is complete. Hidden variables are not motivated by the EPR thought experiment.

than the time scale of free evolution and the latter does not need to be considered.

Results

State preparation before the entangling collision

Figure 1 illustrates the positions and momenta of two particles ‘A’ and ‘B’ at fixed state-preparation time t_0 and at fixed measuring time t_1 . The entangling collision happens at time t_{coll} ($t_0 < t_{\text{coll}} < t_1$) at the position of resting particle A ($\langle \hat{x}_A(t_0) \rangle = 0$). The two bodies are prepared in mutually independent (separable) pure quantum states with Gaussian uncertainties (also shown). Particle A has zero momentum expectation value ($\langle \hat{p}_A(t_0) \rangle = 0$) while its momentum uncertainty is squeezed according to $\Delta^2 \hat{p}_A(t_0) \ll \hbar m_A \Omega / 2$. Its position uncertainty is anti-squeezed according to $\Delta^2 \hat{x}_A(t_0) = \hbar^2 / (4 \Delta^2 \hat{p}_A(t_0))$. Particle B’s position is described by $\langle \hat{x}_B(t_0) \rangle = -x_0$ with a squeezed uncertainty $\Delta^2 \hat{x}_B(t_0) \ll \hbar / (2 m_B \Omega)$. It has a large positive momentum with an anti-squeezed uncertainty according to

$$\langle \hat{p}_B(t_0) \rangle \gg \Delta \hat{p}_B(t_0) = \frac{\hbar}{2 \Delta \hat{x}_B(t_0)} \gg \sqrt{\frac{\hbar m_B \Omega}{2}}. \quad (3)$$

1D-Collision with 50% momentum transfer

Every single collision ‘i’ must obey momentum as well as energy conservation. This leads to the well-known effect that a one-dimensional elastic collision of two bodies with *identical* masses swap their motional quantum states. In this case, the two bodies remain in separable states of motion, and the collision does not produce any entanglement.

Keeping the 1D setting, the situation becomes different if the masses are unequal. The strongest quantum correlation occurs when the prepared bodies have a collision with 50% momentum transfer, as the momentum uncertainties are then also transferred in the same ratio. The momentum transfer is both ways, but only the momentum transfer from B to A is relevant. The other direction is irrelevant because A has zero momentum and negligible momentum uncertainty. The transfer of momentum uncertainty is effectively ‘oneway’. This is what the entanglement produces.

The 50% momentum transfer in Fig. 1 is described by

$$\frac{1}{2} m_B v_{B,i}(t_0) \approx m_B v_{B,i}(t_1) = p_{B,i}(t_1) \quad (4)$$

$$\approx m_A v_{A,i}(t_1) = p_{A,i}(t_1). \quad (5)$$

Energy conservation requires

$$m_B v_{B,i}^2(t_0) \approx m_B v_{B,i}^2(t_1) + m_A v_{A,i}^2(t_1). \quad (6)$$

Combining these equations provides the optimal mass ratio for maximal entanglement of

$$m_B = 3 m_A. \quad (7)$$

Emergent EPR quantum correlations

Eqs. (4), (5) and (6) are justified approximations because particle A has zero momentum and a (strongly) squeezed momentum uncertainty before the collision. No momentum and no kinetic energy is thus transferred from particle A to particle B in course of the elastic collision. Eqs. (4) and (5) readily state that the *momenta of A and B are perfectly correlated* for every individual pair collision ‘i’: A measurement of the momentum $p_{A,i}(t_1)$ allows to precisely infer the momentum $p_{B,i}(t_1)$ and vice versa.

The quantum anti-correlation in the bodies’ positions can be shown by considering their velocities. Eqs. (4), (5) and (7) yield

$$\frac{2}{3} v_{A,i}(t_1) = 2 v_{B,i}(t_1) = v_{B,i}(t_0) \equiv \langle v_B(t_0) \rangle + \delta v_{B,i}(t_0), \quad (8)$$

with $|\delta v_{B,i}(t_0)| \ll |\langle v_B(t_0) \rangle|$, where $\delta v_{B,i}(t_0)$ can be either positive or negative describing the effect of the quantum uncertainty on individual measurement outcomes.

The time of collision t_{coll} has an uncertainty described by

$$\delta t_{\text{coll},i} = \frac{\delta x_{A,i}(t_0)}{\langle v_B(t_0) \rangle + \delta v_{B,i}(t_0)} \approx \frac{\delta x_{A,i}(t_0)}{\langle v_B(t_0) \rangle}. \quad (9)$$

As illustrated by the left circle in the figure of the supplementary information, the position of B according to a single measurement at time t_1 is then approximated by

$$\begin{aligned} x_{B,i}(t_1) &= -x_0 + (\langle v_B(t_0) \rangle + \delta v_{B,i}(t_0)) \\ &\quad \times \left(\frac{3x_0/2}{\langle v_B(t_0) \rangle} + \frac{\delta t_{\text{coll},i}}{2} \right) \\ &\approx \frac{x_0}{2} + \frac{\langle v_B(t_0) \rangle \delta t_{\text{coll},i}}{2} + \frac{3 \delta v_{B,i}(t_0) x_0}{2 \langle v_B(t_0) \rangle} \\ &\approx \frac{x_0}{2} + \frac{\delta x_{A,i}(t_0)}{2}, \end{aligned} \quad (10)$$

where all terms are neglected that are small compared to $\langle v_B(t_0) \rangle \delta t_{\text{coll},i}$.

The position of A at measuring time t_1 of run i reads

$$\begin{aligned} x_{A,i}(t_1) &= (\langle v_B(t_0) \rangle + \delta v_{B,i}(t_0)) \\ &\quad \times \left(\delta t_{\text{coll},i} + \frac{3x_0}{2 \langle v_B(t_0) \rangle} - \frac{3 \delta t_{\text{coll},i}}{2} \right) \\ &\approx \frac{3x_0}{2} - \frac{\delta x_{A,i}(t_0)}{2}. \end{aligned} \quad (11)$$

Thus, it is shown that *the positions of the bodies are quantum anti-correlated*. A measurement of the position $x_{A,i}(t_1)$ allows to precisely infer the position $x_{B,i}(t_1)$. There is no quantum uncertainty in the sum of Eqs. (10) and (11).

Proposal for an implementation with ions

Two ions trapped in a linear Paul trap can move in one dimension and also repel each other. The experiment proposed here requires two ions of different masses, preferably in a ratio of 1:3. Potential candidates are potassium (mass number 39) and caesium (mass number 133). In order to realise the experiment in Fig. 1, the (singly charged) potassium ion (‘A’) must be prepared in a momentum-squeezed state before the elastic collision, and the (singly charged) caesium ion (‘B’) must be prepared in a position-squeezed state. This could for example be realised with superimposed, three-dimensional ion traps that have significantly different trap frequencies. The potassium ion (m_A) is initially in the ground state of a trap potential with a low trap frequency Ω_A at the origin ($\langle x_A(t < t_0) \rangle = 0$). The cesium ion (m_B) is initially found in the ground state of a trap potential with a high trap frequency $\Omega_B \gg \Omega_A$ at the location ($\langle x_B(t < t_0) \rangle = -x_0$). At $t = t_0$, both trap potentials are switched off and the linear Paul trap is activated instead, which strongly forces both ions to move in one dimension and has a trap potential of medium trap frequency Ω_P along the axis. The following therefore applies $\Omega_A < \Omega_P < \Omega_B$. Shortly after the trap frequencies Ω_A and Ω_B are switched off, ion A and ion B have a squeezed momentum or a squeezed position with respect to the new trapping frequency Ω_P according to Eq. (2). To prevent the ion motion from being influenced by the evolution of their wave functions in the new potential, ion B is immediately accelerated towards ion A at high speed and the measurements of either the two locations or the two momenta are performed after the collision. The measurement results show the EPR paradox.

Discussion

Einstein, Podolsky and Rosen concluded from their ‘EPR’ thought experiment that quantum theory is incomplete and that the description of physical systems must be supplemented¹ by what was later called ‘local hidden variables’. However, this possibility was ruled out as part of theoretical and experimental work that began in the 1960s^{2–4,10,28–32} and concluded with the award of the Nobel Prize in Physics in 2022.

In the original EPR thought experiment, the physical process of how the necessary entanglement comes about was missing. I can supplement this with this work. Furthermore, I visualise the generation of the entanglement of the positions and momenta of two particles through a time sequence (Fig. 1). A one-to-one realisation of the original EPR thought experiment thus appears possible for the first time. As the even more important result of my work I consider the insight into how the quantum correlations of EPR entanglement arise. This follows directly from the equations and the illustration presented. EPR entanglement arises from the redistribution of the initial quantum uncertainties under the conditions of energy and momentum conservation. If the initial quantum uncertainties are position- or momentum-squeezed, the redistributions are effectively one-way streets, and quantum correlations and entanglement arise in an easily understandable way.

The generation and measurement of EPR entanglement in this paper refers exclusively to the statement of the original EPR thought experiment, which can be adequately described by quantum states with Gaussian (positive) Wigner functions. In general, Gaussian entanglement together with the measurement of Gaussian variables (here position and momentum) is not suitable for violating a Bell inequality, since this situation can be described with a local deterministic model³³. (This is only possible if one disregards the existence of Heisenberg’s uncertainty principle). However, Gaussian entanglement can make a locally deterministic model entirely impossible if non-Gaussian variables are measured, in particular parity^{34,35}. In the context of quantum information, it is a very interesting question whether it is possible to define parity measurements on the Gaussian EPR entangled states of this paper in such a way that the measurement results violate a Bell inequality. This question is not answered here, but I suspect that it is possible.

Data availability

No datasets were generated or analysed during the current study.

Received: 21 December 2024; Accepted: 24 April 2025;

Published online: 14 May 2025

References

1. Einstein, A., Podolsky, B. & Rosen, N. Can Quantum-Mechanical Description of Physical Reality Be Considered Complete? *Phys. Rev.* **47**, 777–780 (1935).
2. Freedman, S. J. & Clauser, J. F. Experimental Test of Local Hidden-Variable Theories. *Phys. Rev. Lett.* **28**, 938–941 (1972).
3. Aspect, A., Grangier, P. & Roger, G. Experimental Tests of Realistic Local Theories via Bell’s Theorem. *Phys. Rev. Lett.* **47**, 460 (1981).
4. Pan, J.-W. J., Bouwmeester, D., Daniell, M., Weinfurter, H. & Zeilinger, A. Experimental test of quantum nonlocality in three-photon Greenberger-Horne-Zeilinger entanglement. *Nature* **403**, 515–519 (2000).
5. Schrödinger, E. Discussion of Probability Relations between Separated Systems. *Math. Proc. Camb. Philos. Soc.* **31**, 555–563 (1935).
6. Aspect, A., Dalibard, J. & Roger, G. G. Experimental test of Bell’s inequalities using time-varying analyzers. *Phys. Rev. Lett.* **49**, 1804–1807 (1982).
7. Sackett, C. A. et al. Experimental entanglement of four particles. *Nature* **404**, 256 (2000).
8. Rauschenbeutel, A. et al. Step-by-Step Engineered Multiparticle Entanglement. *Science* **288**, 2024–2028 (2000).
9. Jost, J. D. et al. Entangled mechanical oscillators. *Nature* **459**, 683–685 (2009).
10. Hensen, B. et al. Loophole-free Bell inequality violation using electron spins separated by 1.3 kilometres. *Nature* **526**, 682–686 (2015).
11. Riedinger, R. et al. Remote quantum entanglement between two micromechanical oscillators. *Nature* **556**, 473–477 (2018).
12. Ou, Z. Y., Pereira, S. F., Kimble, H. J. & Peng, K. C. Realization of the Einstein-Podolsky-Rosen paradox for continuous variables. *Phys. Rev. Lett.* **68**, 3663–3666 (1992).
13. Bowen, W. P. et al. Experimental investigation of continuous-variable quantum teleportation. *Phys. Rev. A* **67**, 032302 (2003).
14. Aspden, R. S., Tasca, D. S., Boyd, R. W. & Padgett, M. J. EPR-based ghost imaging using a single-photon-sensitive camera. *N. J. Phys.* **15**, 073032 (2013).
15. Kumar, A., Nirala, G. & Marino, A. M. Einstein?Podolsky?Rosen paradox with position?momentum entangled macroscopic twin beams. *Quantum Sci. Technol.* **6**, 045016 (2021).
16. Julsgaard, B., Kozhekin, A. & Polzik, E. S. Experimental long-lived entanglement of two macroscopic objects. *Nature* **413**, 400–3 (2001).
17. Peise, J. et al. Satisfying the Einstein?Podolsky?Rosen criterion with massive particles. *Nat. Commun.* **6**, 1–8 (2015).
18. Giulini, D. On Galilei Invariance in Quantum Mechanics and the Bargmann Superselection Rule. *Ann. Phys.* **249**, 222–235 (1996).
19. Heisenberg, W. Über den anschaulichen Inhalt der quantentheoretischen Kinematik und Mechanik. *Z. f.ür. Phys.* **43**, 172–198 (1927).
20. Kennard, E. H. Zur Quantenmechanik einfacher Bewegungstypen. *Z. f.ür. Phys.* **44**, 326–352 (1927).
21. Weyl, H. Quantenmechanik und Gruppentheorie. *Z. f.ür. Phys.* **46**, 1–46 (1927).
22. Robertson, H. P. The Uncertainty Principle. *Phys. Rev.* **34**, 163–164 (1929).
23. Duan, L., Giedke, G., Cirac, J. & Zoller, P. Inseparability criterion for continuous variable systems. *Phys. Rev. Lett.* **84**, 2722–5 (2000).
24. Simon, R. Peres-Horodecki Separability Criterion for Continuous Variable Systems. *Phys. Rev. Lett.* **84**, 2726 (2000).
25. Reid, M. Demonstration of the Einstein-Podolsky-Rosen paradox using nondegenerate parametric amplification. *Phys. Rev. A* **40**, 913–923 (1989).
26. Händchen, V. et al. Observation of one-way Einstein-Podolsky-Rosen steering. *Nat. Photonics* **6**, 598–601 (2012).
27. Schnabel, R. Squeezed states of light and their applications in laser interferometers. *Phys. Rep.* **684**, 1–51 (2017).
28. Bell, J. S. On the Einstein Podolsky Rosen Paradox. *Physics* **1**, 195–200 (1964).
29. Clauser, J. F., Home, M. A., Shimony, A. & Holt, R. A. Proposed experiment to test local hidden-variable theories. *Phys. Rev. Lett.* **23**, 880 (1969).
30. Clauser, J. F. & Shimony, A. Bell’s theorem: experimental tests and implications. *Rep. Prog. Phys.* **41**, 1881 (1978).
31. Weihs, G., Jennewein, T., Simon, C., Weinfurter, H. & Zeilinger, A. Violation of Bell’s Inequality under Strict Einstein Locality Conditions. *Phys. Rev. Lett.* **81**, 5039–5043 (1998).
32. Giustina, M. et al. Bell violation using entangled photons without the fair-sampling assumption. *Nature* **497**, 227–30 (2013).
33. Bell, J. S. *Speakable and unspeakable in quantum mechanics*. Cambridge University Press, Cambridge, 1987, Chap. 21.
34. Banaszek, K. & Wódkiewicz, K. Nonlocality of the Einstein-Podolsky-Rosen state in the Wigner representation. *Phys. Rev. A* **58**, 4345 (1998).
35. Royer, A. Wigner function as the expectation value of a parity operator. *Phys. Rev. A* **15**, 449–450 (1977).

Acknowledgements

This work was partially performed within the European Research Council (ERC) Project MassQ (Grant No. 339897) and within Germany's Excellence Strategy – EXC 2056 'Advanced Imaging of Matter', project ID 390715994 and EXC 2121 'Quantum Universe', project ID 390833306, which are financed by the Deutsche Forschungsgemeinschaft. R.S. acknowledges financial support from the Open Access Publication Fund of Universität Hamburg. The author thanks Jesse Everett for pointing out that the original illustrations did not match the equations and were wrong.

Author contributions

R.S. developed the research results, wrote the manuscript and the supplementary information, and conceived and produced the figures.

Funding

Open Access funding enabled and organized by Projekt DEAL.

Competing interests

The author declares no competing interests.

Additional information

Supplementary information The online version contains supplementary material available at <https://doi.org/10.1038/s41534-025-01028-7>.

Correspondence and requests for materials should be addressed to Roman Schnabel.

Reprints and permissions information is available at <http://www.nature.com/reprints>

Publisher's note Springer Nature remains neutral with regard to jurisdictional claims in published maps and institutional affiliations.

Open Access This article is licensed under a Creative Commons Attribution 4.0 International License, which permits use, sharing, adaptation, distribution and reproduction in any medium or format, as long as you give appropriate credit to the original author(s) and the source, provide a link to the Creative Commons licence, and indicate if changes were made. The images or other third party material in this article are included in the article's Creative Commons licence, unless indicated otherwise in a credit line to the material. If material is not included in the article's Creative Commons licence and your intended use is not permitted by statutory regulation or exceeds the permitted use, you will need to obtain permission directly from the copyright holder. To view a copy of this licence, visit <http://creativecommons.org/licenses/by/4.0/>.

© The Author(s) 2025, corrected publication 2025